THE JOURNAL OF BIOLOGICAL CHEMISTRY VOL. 291, NO. 49, pp. 25641–25655, December 2, 2016

Fatty Acid Binding to the Allosteric Subunit of Cyclooxygenase-2 Relieves a Tonic Inhibition of the Catalytic Subunit*

Received for publication, September 8, 2016, and in revised form, October 13, 2016 Published, JBC Papers in Press, October 18, 2016, DOI 10.1074/jbc.M116.757310

Liang Dong[‡1], **Chong Yuan**[‡1], **Benjamin J. Orlando**[§1], **Michael G. Malkowski**[§2], **and William L. Smith**[‡3]

From the [‡]*Department of Biological Chemistry, University of Michigan Medical School, Ann Arbor, Michigan 48109 and the* [§]*Department of Structural Biology, University at Buffalo, The State University of New York, and the Hauptman-Woodward Medical Research Institute, Buffalo, New York 14203*

Edited by Dennis Voelker

Prostaglandin endoperoxide H synthase-2 (PGHS-2), also called cyclooxygenase-2 (COX-2), converts arachidonic acid to PGH_2. PGHS-2 is a conformational heterodimer composed of allosteric (E_{allo}) and catalytic (E_{cat}) subunits. Fatty acids (FAs) bind to Arg-120 of E_{allo} increasing to different degrees, depending on the FA, the V_{max} of its E_{cat} partner. We report here that movement of helical residues 120–122 and loop residues 123–129 of E_{allo} underlies the allosteric effects of FAs and allosteric COX-2 inhibitors, including naproxen and flurbiprofen. An S121P substitution in both PGHS-2 monomers yields a variant (S121P/S121P PGHS-2) that has 1.7–1.8 times the V_{max} of native PGHS-2 and is relatively insensitive to activation by FAs or inhibition by allosteric inhibitors. The S121P substitution in E_{allo} is primarily responsible for these effects. In X-ray crystal structures, the Cα atoms of helical residues 119–122 of S121P/S121P PGHS-2 are displaced from their normal positions. Additionally, the S121P/S121P PGHS-2 variants in which Pro-127 and Ser-541 are replaced by cysteines spontaneously forms Cys-127 to Cys-541 cross-links between monomers. This is unlike the corresponding native PGHS-2 variant and suggests that S121P substitutions also unhinge the loop involving residues 123–129. We conclude the following: (*a*) the region involving residues 120–129 of unoccupied E_{allo} tonically inhibits E_{cat}; (*b*) binding of an activating FA (*e.g.* arachidonic, palmitic, or oleic acid) to E_{allo} or an S121P substitution in E_{allo} repositions this region to increase E_{cat} activity; and (*c*) allosteric COX inhibitors act by preventing FA binding to E_{allo} and additionally by relocating E_{allo} residues to inhibit E_{cat}.

Prostaglandin endoperoxide H synthases (PGHSs),[4] also known generically as cyclooxygenases (COXs), convert arachidonic acid (AA), two O_2 molecules and two electrons from an unknown reductant(s) to prostaglandin H_2 (PGH_2) (1, 2). The formation of PGH_2 from AA involves two enzymatic steps. First, the COX activity of PGHSs catalyzes the introduction of two O_2 molecules into the AA backbone forming PGG_2, a bicyclic compound with an endoperoxide group bridging C-9 to C-11 and having a hydroperoxyl group at C-15. This latter group is reduced to an alcohol by the peroxidase (POX) activity of PGHSs in forming PGH_2. PGH_2 is the precursor for enzymes that produce what are considered to be the most important biologically active prostanoids, which include PGD_2, PGE_2, $PGF_{2\alpha}$, PGI_2 (prostacyclin), and thromboxane A_2 (2). There is a functional interplay between the COX and POX sites in that the heme group at the POX site needs to be oxidized by a peroxide to oxidize Tyr-385 in the COX site to a tyrosyl radical. Although apparently not rate-limiting (3), the Tyr-385 radical abstracts the 13-pro-*S*-hydrogen from AA to initiate the COX reaction (1).

PGHSs are homodimers with subunit molecular masses of about 72 kDa (2). Previous studies have established that although PGHSs are sequence homodimers, they function as conformational heterodimers composed of a regulatory allosteric subunit designated E_{allo} and a catalytic subunit denoted E_{cat} (4–12). Compared with E_{allo}, E_{cat} binds heme with high affinity, and maximal activity occurs with one heme/dimer (13–15). The COX-binding sites of E_{allo} and E_{cat} exhibit different binding and functional properties. For example, with both PGHS isoforms, AA binds with higher affinity to E_{allo} than E_{cat}, but AA is only oxygenated by E_{cat} (11, 14, 15). In the case of PGHS-2, numerous fatty acids (FAs), both substrate and non-substrate (ns) FAs, and some nonsteroidal anti-inflammatory drugs (NSAIDs), including ibuprofen (IBP), naproxen, and flurbiprofen (FBP), also bind with higher affinity to E_{allo} than E_{cat} and allosterically regulate E_{cat} activity (5–12, 14). Some FAs

* This work was supported by National Institutes of Health Grants GM077176 (to M. G. M,), GM115386 (to M. G. M.), and GM68848 (to W. L. S.) from NIGMS, Grant CA130810 (to W. L. S.) from NCI, and Grant HL117798 (to W. L. S.) from NHLBI. William L. Smith has served as a consultant for Cayman Chemical Company, products from which were used in this study. The content is solely the responsibility of the authors and does not necessarily represent the official views of the National Institutes of Health.

The atomic coordinates and structure factors (codes 5JVY, 5JW1, and 5JVZ) have been deposited in the Protein Data Bank (http://wwpdb.org/).

[1] These authors contributed equally to this work.

[2] To whom correspondence may be addressed. Tel.: 716-898-8624; Fax: 716-898-8660; E-mail: malkowski@hwi.buffalo.edu.

[3] To whom correspondence may be addressed: Dept. of Biological Chemistry, University of Michigan Medical School, 5301 MSRB III, 1150 W. Medical Center Dr., Ann Arbor, MI 48109-0606. Tel.: 734-647-6180; Fax: 734-763-4581; E-mail: smithww@umich.edu.

[4] The abbreviations used are: PGHS, prostaglandin endoperoxide H synthase; FA, fatty acid; AA, arachidonic acid; βOG, *N*-octyl β-D-glucopyranoside; CPM, 7-diethylamino-3-(4′-maleimidylphenyl)-4-methylcoumarin; EPA, 5,8,11,14,17-*cis*-eicosapentaenoic acid; hu, human; FBP, flurbiprofen; mu, murine; NSAID, nonsteroidal anti-inflammatory drug; IBP, (*S*)-(+)-ibuprofen; mu, murine; ns, non-substrate PA, palmitic acid; PG, prostaglandin; IBP, ibuprofen; POX, peroxidase; PDB, Protein Data Bank.

allosterically stimulate COX activity, whereas IBP, naproxen, and FBP allosterically inhibit activity.

Binding of allosteric ligands involves the interaction of the carboxylate groups of the ligands with the arginino group of Arg-120 of E_{allo} (9, 11). Arg-120 is two residues in from the partially deformed C terminus of helix D of huPGHS-2 (2, 16). The N-terminal end of this helix D forms part of the membrane binding domain of PGHS-2 (17–19). Arg-120 of E_{cat} is also important for ω-3 and ω-6 polyunsaturated FA substrate binding to PGHSs (9, 20–27). This residue lies at the opening of an L-shaped hydrophobic core of the COX active site of E_{cat} (27).

Cross-linking studies with huPGHS-2 (5) and structural studies with ovine PGHS-1 (7, 14, 28) have suggested that ligand binding to Arg-120 of E_{allo} elicits changes in the position of a flexible loop immediately downstream of Arg-120 involving residues 123–129 (Fig. 1). To simplify our presentation, we designate the loop that contains residues 123–129 as the allosteric loop. Repositioning of the allosteric loop upon ligand binding changes its interaction with a region in the partner E_{cat} monomer involving residues 541–543 of E_{cat}. Thus, substitution of residues 126 and 543 or 127 and 541 with cysteines leads to oxidant-induced cross-linking between monomers comprising a dimer. Importantly, the cross-linking can be blocked by ligands that can bind simultaneously to E_{allo} and E_{cat} (5, 11). This suggests that simultaneous binding of E_{allo} and E_{cat} ligands causes a relative repositioning of the allosteric loop.

Although it is clear from studies of huPGHSs in solution that E_{allo} and E_{cat} must be structurally different, X-ray crystallographic studies performed to date have not clearly distinguished E_{allo} from E_{cat}. PGHSs tend to crystallize as symmetric monomers even under conditions in which the ratios of protein monomers to ligand are less than one (28). In a few cases involving a relative excess of FA ligands, FA substrates are found in different orientations in the two subunits of murine (mu) PGHS-2; however, there are no differences in the structures of the bound subunits (27). Additionally, with muPGHS-2, palmitic acid (PA) binds only one of the two subunits, presumably E_{allo}, but there is no difference between the structures of the occupied and unoccupied monomers (14). With ovine PGHS-1, the loop involving residues 121–129 was determined to be in two orientations in a structure showing partial occupancy of one subunit by celecoxib (7) and FBP (Fig. 1*C*) (28). The largest differences in positions between the two orientations of the loops involved residues 123–126. It was for these many reasons that we investigated residues within, adjoining, and interacting with this allosteric loop in huPGHS-2 to learn more about the how E_{allo} regulates E_{cat}. Our enzymologic studies were performed with huPGHS-2, whereas muPGHS-2 was used for the X-ray crystallography. Previous enzymologic studies have been performed with both muPGHS-2 and huPGHS-2, and the results are qualitatively similar (10–12). Until very recently, X-ray crystallographic structures have been reported in the PDB only with muPGHS-2 (29, 30). Crystallographic studies that post-date the structure determinations reported here indicate that the murine and human crystal structures are virtually identical (31).

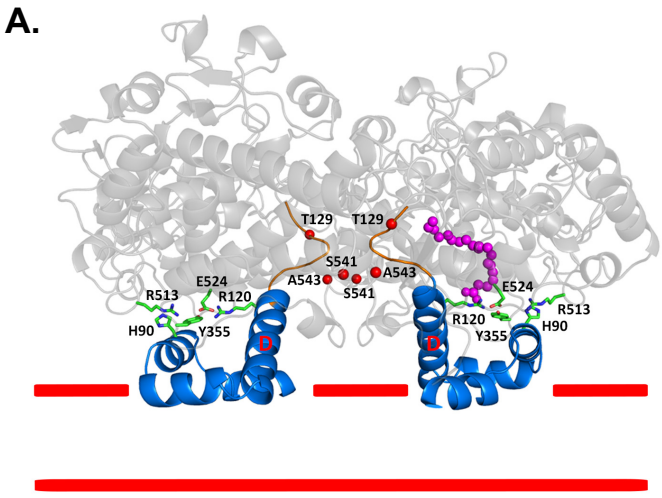

FIGURE 1. **Position, sequence, and structure of the allosteric loop of PGHSs.** *A*, schematic of the PGHS-2 dimer. The membrane binding domain of each monomer is highlighted in *blue*, with helix D labeled and the membrane bilayer denoted by *red lines*. The side chain residues located at the opening of the cyclooxygenase channel in each monomer are shown as *sticks* and labeled accordingly. The allosteric loop is shown in *orange*, with the location of Thr-129 depicted as a *red sphere* (for clarity). Similarly, the location of residues Ser-541 and Ala-543 at the dimer interface are depicted as *red spheres*. AA (*pink*) is shown bound to E_{cat}. *B*, comparison of amino acid sequences of a portion of helix D that extends to residue 122, and the allosteric loop that extends from residue 123 to 129 of PGHS-1 and PGHS-2 from different species (2). *C*, stereoview reproduced from Ref. 28 with permission of the allosteric loop of a flurbiprofen/ovine R120Q/Native PGHS-1 co-crystal structure showing alternative conformations of the allosteric loop with *blue* and *orange sticks* representing the "up" and "down" configurations of amino acids (PDB code 3N8W).

Results

Effects of Substitutions of Residues 120–127 and Neighboring Residues of huPGHS-2—In a first set of experiments, we examined the effects of mutations in the huPGHS-2 dimer (*a*) near the C terminus of helix D, (*b*) in the loop downstream of helix D, (*c*) of Arg-44 which forms a hydrogen bond with Asp-125 of the loop, and (*d*) of Ser-541 and Ala-543 that neighbor this allosteric loop (Fig. 1 and Table 1). Identical mutations were intro-

TABLE 1

Properties of huPGHS-2 variants having substitutions of residues adjoining Arg-120 or in the allosteric loop immediately downstream of Arg-120 or of residues that interact with this loop

huPGHS-2 variants were prepared and purified, and COX activities were assayed as described under "Experimental Procedures." Kinetic values are derived from the average of triplicate determinations that varied by less than ±5% from the average. Measurements of [1-^{14}C]AA binding and displacement of bound [1-^{14}C]AA by PA were performed as described under "Experimental Procedures." ND means not determined.

	COX activity with arachidonic acid					
huPGHS-2 variant	Specific activity (units/mg protein with 100 μM AA or V_{max})	% activity with PA relative to control	% activity with 18:1ω9 relative to control	% activity with 20:1ω9 relative to control	Arachidonic and palmitic acid binding to E_{allo}. [1-^{14}C]AA binding/displacement of bound [1-^{14}C]AA by PA	Comments. nsFA specificity and magnitude of response
Native/Native	36 (43[a])	176[b], 219[c]	134[b], 156[c]	132[b]	Yes/Yes (with 5 μM PA)	Control values to left
R44A/R44A	15[a]	108[d]	155[d]	130[d]	Yes/Yes (with 5 μM PA)	Diminished with PA
R44Q/R44Q	21	95[d]	125[d]	128[d]	Yes/Yes (with 5 μM PA)	Diminished with PA
R120A/R120A[e]	18	92[b]	92[b]	101[b]	No	No effects of nsFA
S121P/S121P	79[a]	120[b], 139[d]	101[b], 118[d]	102[b], 117[d]	Yes/Yes (with 5 μM PA)	Same specificity; overall decreased responses
S121G/S121G	40[a]	ND	ND	ND	ND	ND
H122N/H122N	40	171[b]	135[b]	143[b]	ND	Same as native huPGHS-2
H122P/H122P	23[a]	ND	ND	ND	ND	ND
L123A/L123A	42	125[b]	104[b]	113[b]	ND	Same specificity; decreased response
I124A/I124A	27	125	111[c]	112[c]	ND	Same specificity; decreased response
D125A/D125A	28[a]	125[b]	125[b]	132[b]	ND	Decreased response to PA
D125P/D125P	19	117[d]	118[d]	128[d]	Yes/Yes (with 5 μM PA)	Decreased response to PA
S126C/S126C ΔC[f]	36	ND	ND	ND	ND	ND
P127C/P127C ΔC[f]	32	ND	ND	ND	ND	ND
S541C/S541C ΔC[f]	38	ND	ND	ND	ND	ND
A543C/A543C ΔC[f]	35[a]	ND	ND	ND	ND	ND
A543E/A543E	38	115[b]	155[b]	189[b]	Yes/Yes (with 2.5 μM PA)	Decreased response to PA; increased response of oleic acid and 20:1ω9
A543E H122N/ A543E H122N	43	113[b]	138[b]	153[b]	ND	Decreased response to PA; increased response of oleic acid and 20:1ω9

[a] Number indicates V_{max} value.
[b] Number indicates 5 μM AA + 25 μM nsFA (palmitic acid, oleic acid (18:1ω9) or 20:1ω9).
[c] Number indicates 1 μM AA + 25 μM nsFA (palmitic acid or oleic acid (18:1ω9)).
[d] Number indicates 2 μM AA +25 μM nsFA (palmitic acid, oleic acid (18:1ω9) or 20:1ω9).
[e] Data are from Ref. 9.
[f] Data are from Ref. 5.

duced into both monomers by substituting alanine and/or the amino acid present at the corresponding position of PGHS-1. Note that because the mutations are in both subunits of the huPGHS-2 dimer, the results observed are a composite of effects occurring in both E_{allo} and E_{cat}.

As reported previously, substitution of Arg-120 with alanine abrogates the allosteric effects of PA, oleic acid, and 20:1ω9 that are not COX substrates (*i.e.* non-substrate fatty acids (nsFAs)) (Table 1) (9). This is because FAs do not efficiently bind to E_{allo} of R120A/R120A huPGHS-2. Moreover, E_{cat} of this mutant binds AA with a 5–10-fold lower affinity than does E_{cat} of native huPGHS-2 (9).

S121P/S121P huPGHS-2 has quite different properties than native huPGHS-2, notably an almost 2-fold higher specific COX activity with AA (Table 1). S121P/S121P huPGHS-2 also exhibited substantially diminished allosteric responses to PA, oleic acid, and 20:1ω9. PA caused a modest 20% allosteric activation of S121P/S121P huPGHS-2 compared with a 75% activation of native huPGHS-2 under the same conditions. Other amino acid substitutions intended to destabilize the N terminus of helix D either had no effect on COX activity (*i.e.* S121G) or significantly decreased COX activity (*i.e.* H122P). A relatively neutral H122N substitution had little effect on huPGHS-2.

Substitutions of allosteric loop residues 123, 124, and 125 diminished allosteric responses to PA and oleic acid. Residue 543, which neighbors residue 126 in huPGHS-2 (5), is a glutamate in PGHS-1 and an alanine in PGHS-2 (2). A543E substitutions reduced the response to PA but had no effect on the response to oleic acid and even enhanced the response to 20:1ω9.

The binding of [1-^{14}C]AA and -PA to E_{allo} was estimated using the method developed previously (14) and described under "Experimental Procedures" that takes advantage of the ability to measure binding at high enzyme to substrate ratios of unreacted [1-^{14}C]AA to E_{allo} of huPGHS-2. Except with R120A/R120A huPGHS-2, [1-^{14}C]AA binding to E_{allo} of the mutants tested in Table 1 was comparable with that observed for E_{allo} of native huPGHS-2 (9). Details are provided below. Although not definitive, the results in Table 1 are consistent with the idea that several of the residues tested, except perhaps His-122, contribute to the allosteric regulation of huPGHS-2 by nsFAs and thus, we suspected, in various ways to the positioning of the allosteric loop.

Characterization of S121P Substituted PGHS-2—The most pronounced effect we observed in testing the mutants shown in Table 1 was the heightened activity of the huPGHS-2 variant having S121P substitutions. This led us to characterize this mutation in detail. Initially, we examined S121P/S121P huPGHS-2, which carries the S121P substitution in both subunits. We then analyzed mutants having this substitution individually in E_{allo} or E_{cat}.

Fig. 2 and Table 2 provide comparisons of the specific activities of native huPGHS-2 *versus* S121P/S121P huPGHS-2 with a variety of polyunsaturated FA substrates. S121P/S121P huPGHS-2 had markedly increased activity with AA and somewhat increased activity with dihomo-γ-linolenic acid. There were no appreciable effects caused by the S121P substitution on the K_m values for these two ω6 FA substrates. In contrast, this

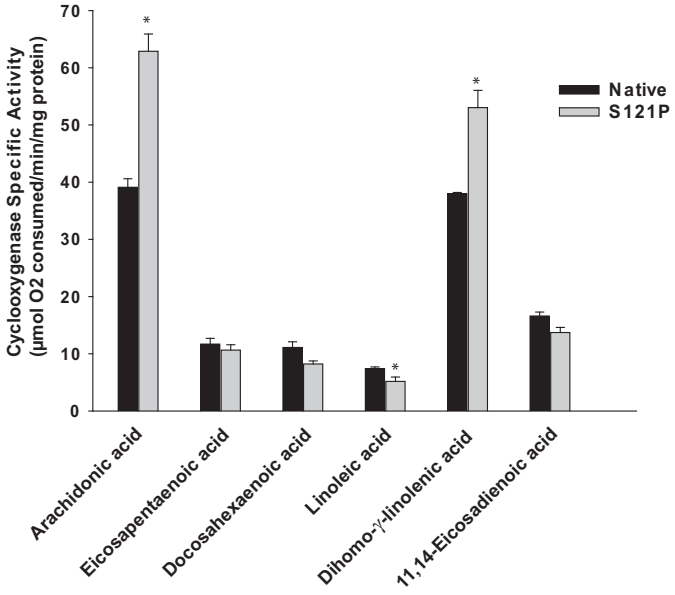

FIGURE 2. **Oxygenation of fatty acid substrates by native huPGHS-2 and S121P/S121P huPGHS-2.** Recombinant enzymes were prepared, and measurements of COX activities using an O_2 electrode were performed with 100 μM concentrations of the indicated fatty acids as noted under "Experimental Procedures." The *error bars* indicate the average ± S.E. A significant difference from the value with the Native/Native (*versus* S121P/S121P) huPGHS-2 as determined by the Student's *t* test ($p < 0.05$) is indicated with an *asterisk*. The experiment was performed with two different preparations of enzymes with the same results.

mutant enzyme had somewhat reduced activity toward a variety of other substrates tested, including docosahexaenoic acid, linoleic acid, and 11,14-eicosadienoic acid; in the case of 11,14-eicosadienoic acid, there is a significant increase in the K_m value. None of these latter three substrates efficiently bind to E_{allo} of native huPGHS-2 (11). S121P/S121P huPGHS-2 had essentially the same activity as native huPGHS-2 with 5,8,11,14,17-*cis*-eicosapentaenoic acid (EPA). EPA is an unusual PGHS-2 substrate. Although it does bind to E_{allo} of native huPGHS-2 (11), binding of EPA to E_{allo} of native huPGHS-2 appears to suppress its own oxygenation.[5]

When incubated with [1-^{14}C]AA, S121P/S121P huPGHS-2 formed about the same proportion of PGH_2-derived products as native huPGHS-2 (*i.e.* 89% *versus* 84% for native and S121P/S121P huPGHS-2, respectively; data not shown). Thus, the S121P substitution does not cause a change in the PG product profile. When titrated with heme, S121P/S121P huPGHS-2 exhibited one high affinity heme-binding site with a $K_d = 0.36 \pm 0.07$ μM (data not shown). This value is about twice that originally determined for huPGHS-2, but the same as that we previously determined for Y385F/Native huPGHS-2 (9).

A $K_d = 0.44$ μM was determined for [1-^{14}C]AA binding to S121P/S121P huPGHS-2, which represents binding to the E_{allo} subunit (Table 3). Also, as indicated in Table 3, bound [1-^{14}C]AA was effectively displaced by 5 μM PA. The data

[5] COX activity toward EPA is the same with native huPGHS-2 and Y385F/Native huPGHS-2 (9) but is increased about 2-fold with R120A Y385F/Native huPGHS-2 (L. Dong and W. L. Smith, unpublished data). E_{allo} of the latter variant does not bind EPA (11) suggesting that EPA binding to E_{allo} suppresses COX activity toward EPA.

TABLE 2

Kinetic properties of native and S121P/S121P huPGHS-2 with several ω6 fatty acids that are COX substrates

huPGHS-2 variants were expressed and purified, and COX activities were assayed using an O_2 electrode assay as described under "Experimental Procedures." Kinetic values are derived from the average of triplicate determinations ± S.D. The experiments were performed two different enzyme preparations with comparable results.

Fatty acid substrate	Native huPGHS-2		S121P/S121P huPGHS-2	
	V_{max}	K_m	V_{max}	K_m
	units/mg protein	μM	*units/mg protein*	μM
11,14-Eicosadienoic acid (11,14–20:2ω6)	21 ± 0.4	7.5 ± 1.3	17 ± 0.6	27 ± 6.3
Dihomo-γ-linolenic acid (8,11,14–20:3ω6)	56 ± 2.6	16 ± 3.0	63 ± 3.0	12 ± 2.1
Arachidonic acid (5,8,11,14–20:4ω6)	39 ± 2.1	9.1 ± 1.6	65 ± 3.7	8.9 ± 1.4

TABLE 3

Oxygenation of [1-^{14}C]AA by S121P/S121P huPGHS-2 variants at high enzyme to AA ratios

[1-^{14}C]AA (1 μM) was incubated with the indicated concentration of the huPGHS-2 variant form at 37 °C for 8 min; the reactions were stopped, and the radioactive products and unreacted AA were separated by radio-HPLC and quantified as described under "Experimental Procedures." The results show the percentage of the original [1-^{14}C]AA remaining.

Reaction components	Unreacted [1-^{14}C]arachidonic acid remaining after 8 min (% of starting radioactivity)			
	Replicate 1	Replicate 2	Replicate 3	Average ± S.D.
0.1 μM S121P/S121P huPGHS-2 + 1 μM [1-^{14}C]AA	6.55	5.25		5.9 ± 0.9
2 μM S121P/S121P huPGHS-2 + 1 μM [1-^{14}C]AA	11.1	12.93	12.47	12 ± 1.0[a]
2 μM S121P/S121P huPGHS-2 + 1 μM [1-^{14}C]AA, then after 4 min added 20 μM unlabeled AA	5.85	5.54		5.7 ± 0.2
2 μM S121P/S121P huPGHS-2 + 1 μM [1-^{14}C]AA, then after 4 min added 5 μM PA	6.93	6.03		6.5 ± 0.6

[a] Significant difference from value with 0.1 μM enzyme as determined using a Student's *t* test ($p < 0.05$) is shown.

TABLE 4

Crystallographic statistics

NA means not applicable.

Crystallographic parameter	S121P/apo	S121P/cbx	S121P/fbp
Space group	*I*222	*I*222	*I*222
No. in asymmetric units	2	2	2
Unit cell length (Å)			
a	121.10	120.36	119.92
b	131.93	132.2	131.59
c	180.32	180.39	179.98
α = β = γ (°)	90.00	90.00	90.00
Wavelength (Å)	1.0000	1.0000	1.0000
Resolution (Å)	30–2.36	30–2.82	30–2.62
Highest resolution shell (Å)	2.40–2.36	2.87–2.82	2.67–2.62
R_{merge}[a]	8.6 (64.5)[b]	10.3 (70.5)	9.0 (79.4)
R_{meas}	9.9 (74.5)	12.0 (82.0)	10.2 (90.0)
R_{pim}	4.7 (36.8)	5.9 (40.8)	4.8 (41.5)
$CC^{1/2}$	79.0[c]	69.8	69.4
CC^*	94.0	90.7	90.5
Total observations	248,417	126,931	18,871
Total unique	59,557	34,837	43,042
$I/\sigma(I)$	16.6 (2.1)	11.8 (1.9)	15.3 (1.8)
Completeness (%)	99.6 (98.1)	97.8 (98.9)	99.8 (99.8)
Redundancy	4.2 (3.8)	3.7 (3.7)	4.4 (4.5)
No. of reflections in refinement	59,221	32,495	40,667
No. of atoms in refinement	9640	9168	9431
R	16.91	18.92	18.16
R_{free}	21.43	22.63	22.92
Average *B* factor, protein (Å^2)	47.3	42.3	38.9
Average *B* factor, ligand (Å^2)	NA	42.5	37.8
Average *B* factor, solvent (Å^2)	46.8	36.0	34.8
Mean positional error (Å)	0.275	0.360	0.310
r.m.s.d.[d] bond length (Å)	0.003	0.005	0.003
r.m.s.d. bond angle (°)	0.700	0.760	0.710
Ramachandran Plot			
Allowed (%)	97.00	96.00	97
Generous (%)	3.00	3.82	2.91
Disallowed (%)	0.00	0.18	0.09

[a] R_{merge}, R_{meas}, and R_{pim} calculated as described in Ref. 56.
[b] Values in parentheses are for the outermost resolution shell.
[c] $CC^{1/2}$ and CC^* calculated as described in Ref. 57.
[d] r.m.s.d. is root mean square deviation.

establish that although the magnitude of allosteric activation of this variant by PA was less than a third of that seen with native huPGHS-2, E_{allo} of S121P/S121P huPGHS-2 binds AA and PA with similar affinities as native enzyme (Table 4).

Structural Studies of Murine and Human S121P/S121P PGHS-2—As noted in the Introduction, Ser-121 is located near the end of helix D of the membrane-binding domain, adjacent to Arg-120 at the opening of the COX channel. Arg-120, along with Tyr-355 and Glu-524 collectively form a water-mediated interaction network at the channel entrance to effectively bury substrates and inhibitors within the catalytic domain (17, 18, 22, 27, 32). As these interactions decrease the aperture of the channel entrance when ligand is bound, the conformation of COX in this state is generally referred to as the "closed" conformation (33). In addition to forming the constriction, these residues participate in the binding of acidic time-dependent inhibitors and substrates (18, 27, 32, 34–39).

We determined the crystal structure of S121P/S121P muPGHS-2 in the absence of ligands (S121P/apo) bound in the COX channel using synchrotron radiation (Table 4 and Fig. 3). S121P/apo crystallized with two monomers in the asymmetric unit, with complete conservation of the global domain architecture observed in other crystal structures of muPGHS-2 (14, 27, 29). The root mean square deviation calculated between monomers is less than 0.22 Å, smaller than the mean positional error and indicating that there are no significant structural deviations between monomers. Closer inspection of the COX channel opening in the S121P/apo-crystal structure reveals that the S121P mutation disrupts the last helical turn of helix D, causing it to unwind (Fig. 3*A*). As a result, the side chain of Arg-120 is displaced and becomes disordered, as evidenced by the lack of electron density observed beyond the Cβ carbon of the side chain. The 3 Å positional displacement of the main chain in this area of helix D (Fig. 4), in comparison with its position in native enzyme crystal structures complexed with substrates and inhibitors, results in the breakage of the ionic interaction between the side chains of Arg-120 and Glu-524 (Fig. 3). The loss of the Arg-120/Glu-524 ionic interaction

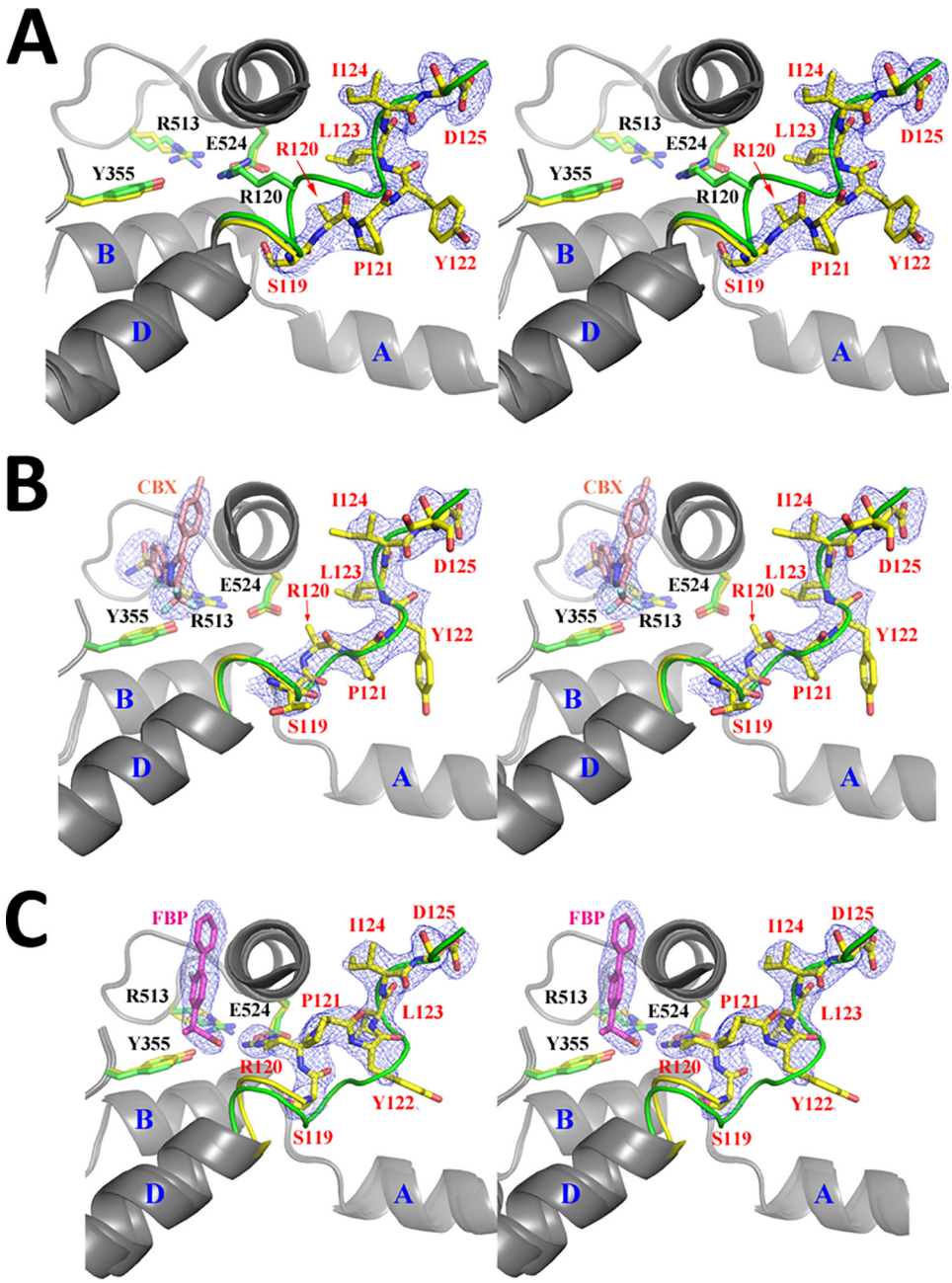

FIGURE 3. **Conformational differences between residues Ser-119 and Asp-125 in the absence and presence of inhibitor.** Stereo views that highlight the main chain conformational differences for residues Ser-119 through Asp-125 at the entrance of the cyclooxygenase channel in the crystal structures of S121P/S121P muCOX-2 in the absence and presence of bound inhibitor. *A,* comparison between the S121P/apo-crystal structure and native muCOX-2 (PDB code 3HS5) depicting the unwinding of the last turn of helix D. Carbon, oxygen, and nitrogen atoms for residues Ser-119 through Asp-125 are colored *yellow*, *red*, and *blue*, respectively. A *green ribbon* depicts the location of the Cα positions for the equivalent residues in the wild type muCOX-2 crystal structure. *B,* comparison between the S121P/apo- and S121P/cbx and *C,* S121P/apo- and S121P/fbp crystal structures highlighting the fact that the binding of FBP induces a rewinding of the last turn of helix D, whereas the binding of celecoxib does not. For all three panels, $F_o - F_c$ simulated annealing omit electron density is shown in *blue mesh* contoured at 2.5σ. The side chains for Tyr-355, Arg-513, and Glu-524, which participate in the water-mediated interaction network at the channel entrance and membrane-binding domain helices A, B, and D, are also labeled accordingly.

results in the opening of the constriction at the base of the COX channel.

R120A/R120A and R120Q/R120Q PGHS-2 constructs are refractory to inhibition by carboxylic acid containing NSAIDs (9, 21, 39). Given the large observed displacement of Arg-120 in the S121P/apo-crystal structure, we hypothesized that NSAIDs requiring an interaction with Arg-120 would not bind to S121P/S121P muPGHS-2. To test this hypothesis, we employed a thermal shift assay to monitor the binding of FBP, IBP, naproxen, and celecoxib to native, R120A/R120A, and S121P/S121P muPGHS-2 variants (Fig. 5). With the exception of celecoxib, all the drugs form an ionic interaction with Arg-120 to facilitate binding. Melting temperatures (T_m) were calculated for all three constructs in the absence and presence of inhibitor. The change in T_m (ΔT_m) was then calculated to provide a measure of inhibitor binding. As expected, all of the drugs bound to native muPGHS-2, inducing ΔT_m shifts of 10–17 °C. Conversely, FBP, IBP, and naproxen failed to induce a significant ΔT_m shift when

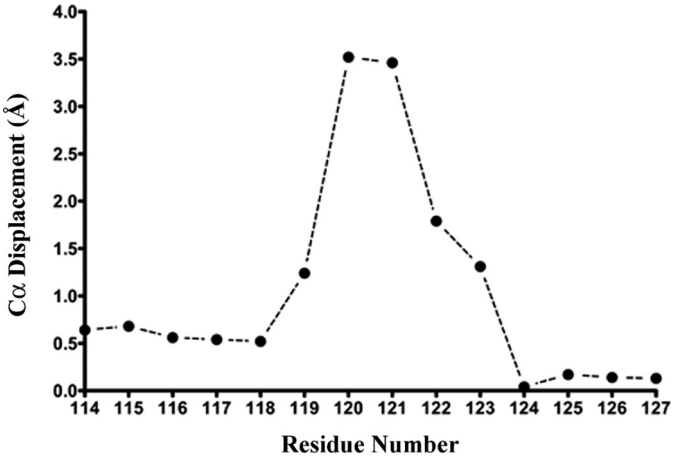

FIGURE 4. **Positional displacement of helix D residues in the S121P/apo-crystal structure.** The plot shows the positional displacement of Cα atoms for residues 114–127 in and around helix D of the membrane-binding domain in the S121P/apo-crystal structure compared with the equivalent residues in the wild type crystal structure bound with AA (PDB code 3HS5).

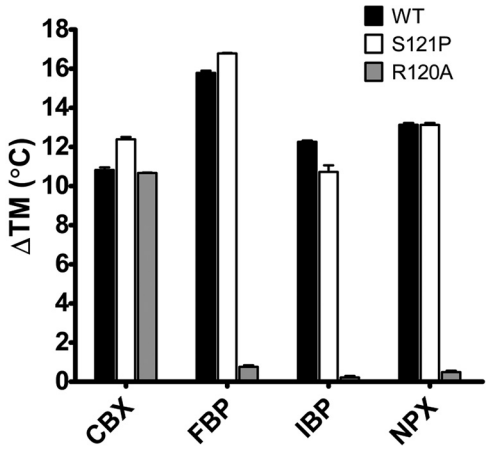

FIGURE 5. **Thermal melting shifts induced by ligand binding to muCOX-2.** Wild type, R120A, and S121P muCOX-2 constructs were incubated with the indicated inhibitor on ice for 30 min, followed by determination of the protein denaturation temperature as described under "Experimental Procedures." Results are reported as the change in melting temperature (ΔT_m) between liganded and unliganded states. Melting temperature measurements were made in triplicate. *CBX* is celecoxib; *NPX* is naproxen.

tested with the R120A/R120A muPGHS-2 construct (Fig. 5). Surprisingly, we observed ΔT_m shifts for all the drugs when tested with the S121P/S121P muPGHS-2 variant, suggesting that inhibitor binding can rescue or reverse the observed displacement of Arg-120 in the S121P/S121P muPGHS-2 mutant.

To follow up on our thermal shift assay observations, we determined the crystal structures of S121P/S121P muPGHS-2 in complex with FBP (S121P-fbp) and celecoxib (S121P-cbx) (Fig. 3). Importantly, NSAID-bound structures were obtained by soaking crystals of the unliganded S121P/S121P muPGHS-2 in cryoprotectant containing 1 mM inhibitor. As with the S121P/apo-crystal structure, the liganded structures exhibited the same domain architecture as other PGHS-2 crystal structures, with no differences between monomers. Celecoxib binds within the cyclooxygenase channel of the S121P/S121P muPGHS-2 with its phenyl sulfonamide moiety inserted into the COX-2 side pocket, analogous to that observed in the native crystal structure (40). Moreover, celecoxib binding fails to induce a rewinding of the last turn of helix D, which exhibits the same conformation observed in the S121P/apo structure. Consistent with our thermal shift assay results and the crystal structure of the native enzyme, there are no interactions between the inhibitor and the side chain of Arg-120 (Fig. 3*B*). FBP also binds within the cyclooxygenase channel of the S121P construct in the same conformation as that observed in the native structure, with its carboxylate moiety forming ionic interactions with the side chain of Arg-120 (18, 41). Importantly, the binding of FBP within the COX channel of the S121P construct results in the rewinding of the last turn of helix D and ordering of the Arg-120 side chain, thus restoring the closed conformation of the channel opening (Fig. 3*C*). Although crystal structures of the S121G and H122P mutants were not determined, we assume based on analysis of the huPGHS-2 variants (Table 4) that neither caused the degree of distortion of helix D that is observed with S121P/S121P muPGHS-2.

The structure of the region involving residues 124–129 is relatively unaltered in any of the crystal structures; however, crystal contacts present in this region of the protein likely constrain movement in the loop that could occur in solution. Therefore, we performed the cross-linking studies depicted in Fig. 6 to test for movement of this allosteric loop. As discussed next, the results provide evidence that at least part of the allosteric loop involving residues 123–129 is repositioned in S121P/S121P huPGHS-2 in solution.

We had previously examined a cysteine-less huPGHS-2 variant denoted P127C A541C Δ*C* huPGHS-2 in which the free cysteines of huPGHS-2 were replaced with serine residues, and new cysteine residues were introduced in the allosteric loop at residue 127 and in an adjoining loop at residue 541 from the partner subunit (5). Addition of an oxidizing agent, a cuprous·*o*-phenanthroline complex, caused a time-dependent cross-linking of the monomers comprising P127C A541C Δ*C* huPGHS-2. This is illustrated for comparison purposes in the *top panel* of Fig. 6 that we previously presented in Ref. 5. The uppermost band is a dimer having two disulfide cross-links; immediately below this is a band having one cross-link, and the lowest band is the monomer (see Ref. 5). The cross-links are between Cys-127 and Cys-541. Cross-linking could be prevented by certain FAs or COX inhibitors that bind both monomers, and we infer that binding of these ligands prevents close apposition of Cys-127 and Cys-541 (5, 11). In the experiment depicted in Fig. 6*A*, formation of cross-linked monomers having one or two disulfide linkages is inhibited by FBP. Note that in the *top panel* at 0 time (Fig. 6) that about two-thirds of the control P127C A541C Δ*C* huPGHS-2 template has become spontaneously cross-linked during expression and purification and prior to the addition of oxidant. We introduced R120Q or S121P substitutions into the P127C A541C Δ*C* huPGHS-2 homodimer template to form the homodimeric variants denoted as R120Q P127C A541C Δ*C* huPGHS-2 (Fig. 6*B*) and S121P P127C A541C Δ*C* huPGHS-2 (Fig. 6*C*). Both of these latter proteins underwent spontaneous cross-linking during their preparation. With R120Q P127C A541C Δ*C* huPGHS-2, which likely binds FBP only weakly (9), spontaneous cross-linking, although very substantial, was not quite complete. Not surprisingly, FBP was relatively ineffective in preventing oxidant-induced cross-linking.

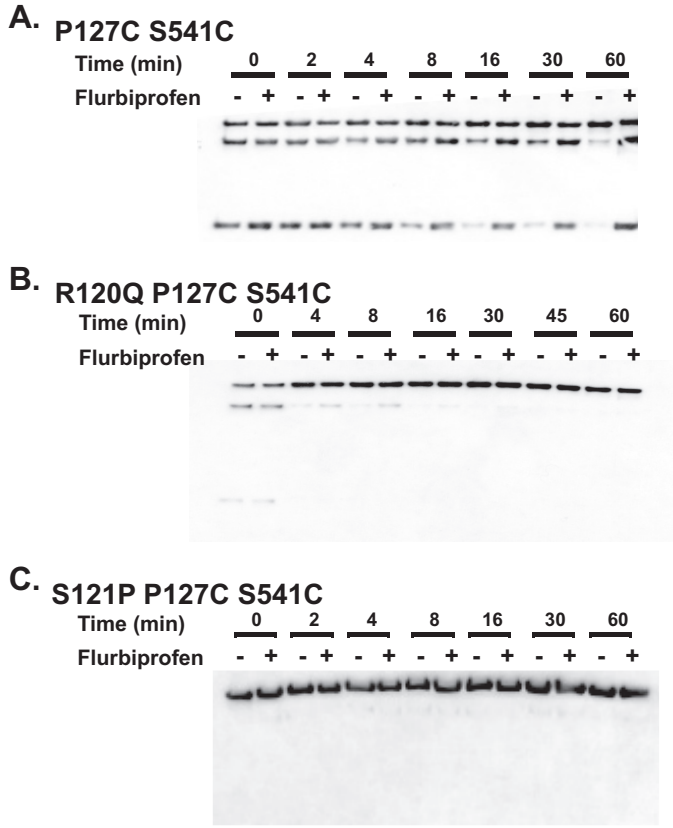

FIGURE 6. **Cross-linking between monomers of P127C S541C Δ*C*-huPGHS-2, R120Q P127C S541C Δ*C*-huPGHS-2, and S121P P127C S541C Δ*C*-huPGHS-2.** The mutant proteins indicated in *panels A*, *B*, and *C* are P127C S541C ΔC-huPGHS-2, R120Q P127C S541C ΔC-huPGHS-2, and S121P P127C S541C ΔC-huPGHS-2, respectively. These recombinant proteins were expressed in a baculovirus system, purified, and subjected to cross-linking by treatment with Cu^{2+}/*o*-phenanthroline for the indicated times in the presence or absence of 100 μM FBP as described under "Experimental Procedures." Samples were subjected to SDS-PAGE in the absence of a disulfide reducing agent (*i.e.* dithiothreitol), and Western blotting was performed using an anti-PGHS-2 antibody.

In the case of S121P P127C A541C Δ*C* huPGHS-2, all the monomers spontaneously cross-linked. We were unable to prevent the complete spontaneous cross-linking even by adding the reversible COX inhibitor IBP to the insect cell culture medium during expression of S121P P127C A541C Δ*C* huPGHS-2.

We interpret the results with R120Q P127C A541C Δ*C* huPGHS-2 as indicating that the Gln-120-containing mutant cannot bind endogenous ligands efficiently (9) and thus that during its preparation the R120Q P127C A541C Δ*C* huPGHS-2 variant is not in a ligand-bound or closed conformation in which cross-linking is prevented. We interpret the results of cross-linking studies with S121P P127C A541C Δ*C* huPGHS-2 to indicate that the S121P substitution leads to the allosteric loop, in this case with the P127C replacement, to be more flexible than in the native protein allowing it to neighbor and cross-link to the adjoining loop containing residue Cys-541.

Effects of S121P Substitutions in E_{allo} Versus E_{cat} of huPGHS-2—To determine how the S121P substitution enables the large increase in V_{max} of huPGHS-2, we characterized mutants having alterations of Ser-121 and other amino acids in either E_{allo} or E_{cat}. As illustrated in Fig. 7, substitutions were introduced into a huPGHS-2 heterodimer variant denoted as Y385F/Native huPGHS-2. This latter variant has a catalytically inactive monomer E_{allo} with a Y385F substitution and a cat-

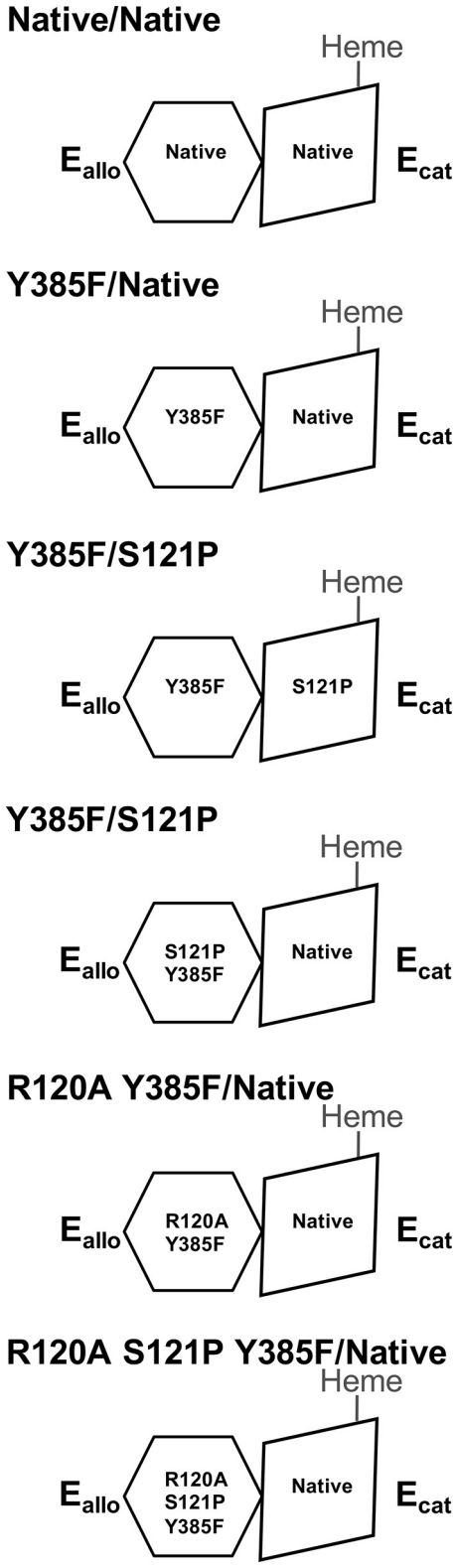

FIGURE 7. **Schematic of heterodimer mutants used to determine the effects of S121P and R120A substitutions in E_{allo} *versus* E_{cat} of huPGHS-2 conformational heterodimer.** Heme has a marked preference for binding the native subunit *versus* a subunit having a Y385F substitution (9). An intact Tyr-385 and bound heme are necessary for COX activity.

TABLE 5

Properties of huPGHS-2 variants having S121P substitutions in E_{allo} *versus* E_{cat} subunits

huPGHS-2 variants were prepared, expressed, and assayed for COX activities with AA as substrate as described previously and under "Experimental Procedures" (9). Increases in COX activity due to PA were measured using 5 μM AA and 25 μM PA. Relative responses to inhibitors were determined after preincubating the huPGHS-2 variants for 30 min with naproxen (0, 1, 2.5, 5, and 25 μM), flurbiprofen (0, 1, 2.5, 5.0, and 25 μM), diclofenac (0, 1, 2, 3, 4, and 8 μM), or celecoxib (0, 0.5, 1, 2, 5 and 15 μM). ND means not determined.

Subunit composition (E_{allo}/E_{cat})	COX V_{max}	COX K_m	% activity with PA relative to control	Relative response to naproxen	Relative response to flurbiprofen	Relative response to diclofenac	Relative response to celecoxib
	units/mg	μM					
Native/Native[a]	43 ± 1.7	9.3 ± 1.0	183 ± 1.0	Control[b]	Control[b]	Control[b]	Control[b]
S121P/S121P	79 ± 4.3	13.8 ± 2.3	136 ± 2.2	Attenuated[b]	Attenuated[b]	Unchanged[c]	Unchanged[c]
Y385F/Native[a]	37 ± 1.3	5.5 ± 0.8	146 ± 3.0	Control[c]	Control[c]	Control[c]	Control[c]
Y385F/S121P	50 ± 1.9	19.3 ± 2.1	148 ± 1.4	Unchanged[c]	ND	ND	Unchanged[c]
S121P Y385F/Native	69 ± 2.0	15.6 ± 1.3	125 ± 3.8	Attenuated[c]	Attenuated[c]	Unchanged[c]	Attenuated[c]
R120A Y385F/Native[a]	16 ± 0.5	10 ± 1.0	103 ± 10	Attenuated[c]	Attenuated[c]	ND	Unchanged[c]
R120A S121P Y385F/Native	54 ± 1.8	8.2 ± 1.0	102 ± 5.3	Attenuated[c]	ND	ND	Attenuated[c]

[a] Data are from Ref. 9.
[b] Data are compared with Native/Native huPGHS-2.
[c] Data are compared with compared to Y385F/Native huPGHS-2.

alytically active monomer E_{cat} that is the native subunit (9). We established that 90% of E_{cat} is the native subunit and remains in this form during the life of the protein (9). S121P and other amino acid substitutions were made in either E_{allo}, the subunit with the Y385F substitution, or the native E_{cat} subunit.

Results comparing Y385F/Native huPGHS-2 with S121P mutants in this background are presented in Table 5. At least two-thirds of the increase in the V_{max} of the S121P/S121P huPGHS-2 is attributable to the S121P substitution in E_{allo}; however, the S121P substitution in E_{cat} also contributes at least in some way to the increase in V_{max} (Table 5). S121P Y385F/Native huPGHS-2 has 85% more activity than Y385F/Native huPGHS-2. This is an increase almost identical to the relative increase observed in comparing S121P/S121P huPGHS-2 to native huPGHS-2. Y385F/S121P huPGHS-2 also exhibits a 35% increase in activity over Y385F/Native huPGHS-2 suggesting that a S121P mutation in E_{cat} also contributes to the enhanced activity observed when this substitution is in both monomers (*i.e.* with S121P/S121P huPGHS-2).

As might be expected were the S121P substitution partially replacing the allosteric stimulation of huPGHS-2 by FAs, Y385F S121P/Native huPGHS-2 was less sensitive to allosteric stimulation by PA than was the Y385F/S121P mutant (Table 5). In contrast, the relative increases in activity with PA were the same for the Y385F/Native huPGHS-2 control and Y385F/S121P huPGHS-2 where the S121P substitution is in E_{cat}.

As summarized in Table 5 the magnitudes of allosteric inhibition of Y385F S121P/Native huPGHS-2 by naproxen and FBP were both decreased in comparison with Y385F/Native and Y385F/S121P huPGHS-2. These two NSAIDs function as allosteric inhibitors of huPGHS-2. In contrast, inhibition by diclofenac, a COX inhibitor that functions by competing for E_{cat} (14), was unaffected in a test of S121P Y385F/Native huPGHS-2. Results comparing dose responses of native huPGHS-2 and S121P Y385F/Native huPGHS-2 to these three inhibitors are presented in Fig. 8. Celecoxib inhibits huPGHS-2 by competing directly with AA for binding to E_{cat}. As noted above, celecoxib inhibition does not involve its binding to Arg-120 in E_{cat}. Thus, we were surprised to find that inhibition by celecoxib was attenuated in huPGHS-2 variants having S121P substitutions in E_{allo} (*i.e.* S121P Y385F/Native and R120A S121P Y385F/Native huPGHS-2). Presumably, Ser-121 in E_{allo} contributes in some way to celecoxib interactions with E_{cat} so as to decrease the inhibitory effect of celecoxib on E_{cat}.

We also compared R120A S121P Y385F/Native to R120A Y385F/Native huPGHS-2 (Table 5). R120A Y385F/Native huPGHS-2 is unable to bind and thus unable to respond to allosteric effectors, including nsFAs and naproxen (9, 14). When introduced into this background, a S121P substitution in E_{allo} increases the V_{max} by more than 3-fold from 16 to 54 units/mg. This is consistent with the idea that the S121P substitution in E_{allo} acts largely by supplanting allosteric responses to AA itself, nsFAs, and allosteric COX inhibitors.

Effects of Substitutions of Asp-125 and Arg-44 on huPGHS-2—Residue 125 is the one residue in the allosteric loop that differs between PGHS-1 and PGHS-2. (*i.e.* Pro-125 in huPGHS-1 *versus* Asp-125 in huPGHS-2 (Fig. 1)). We substituted Asp-125 in both E_{allo} and E_{cat} of huPGHS-2 with proline or alanine to determine the effect of altering this isoform-specific residue in the allosteric loop. We made parallel substitutions of Arg-44 with glutamine or alanine because Arg-44 residue appears to form a hydrogen bond with Asp-125 in muPGHS-2 crystal structures (14, 29). We examined the effect of the various Asp-125 and Arg-44 mutations on basic kinetic parameters and responses to various FAs and to naproxen. The data are presented in summary form in Table 6. Overall, the results of studies of the D125A and R44A mutants show reductions in V_{max} values with little or no changes in either K_m values or in the affinities of AA or PA for E_{allo}. In several cases, mutations in either E_{allo} or E_{cat} substantially reduced the V_{max} values but to levels significantly lower than those seen with the mutations in both E_{allo} and E_{cat}. Comparison of the data obtained with these mutants indicated that both Asp-125 and Arg-44 contribute to the functioning of both E_{allo} and E_{cat}. Thus, we could not make definitive conclusions about the role of these residues in the individual monomers. We did note that with either D125A or R44A substitutions in E_{allo} but not E_{cat} that there were decreases in the allosteric responses to both PA and naproxen. However, the patterns seen with D125A and R44A were different from the ones observed with D125P or R44Q substitutions. We observed that values for basic kinetic parameters with enzymes having D125A substitutions were not mark-

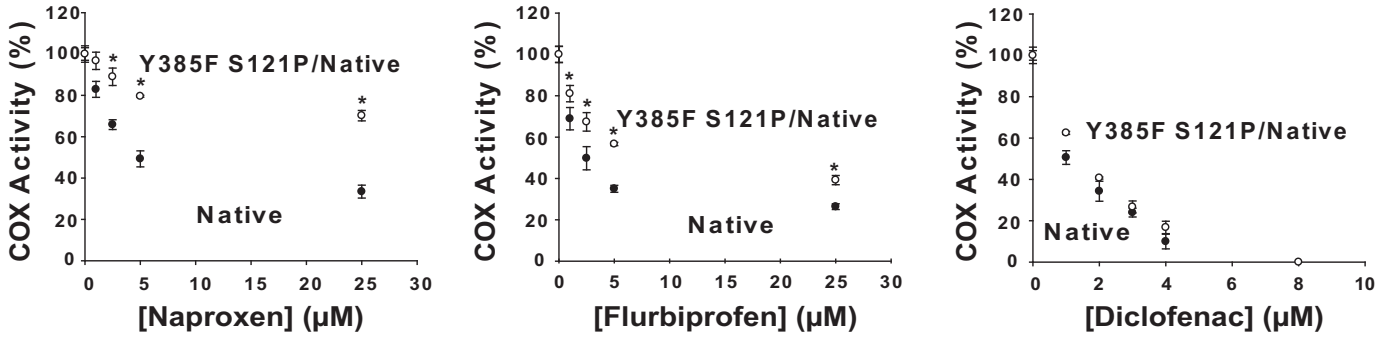

FIGURE 8. **Inhibition by naproxen, flurbiprofen, and diclofenac of Native/Native huPGHS-2 compared with the Y385F S121P/Native huPGHS-2 heterodimer.** In the Y385F S121P/Native huPGHS-2 heterodimer, the S121P is in the E_{allo} subunit as illustrated in Fig. 7. The indicated purified huPGHS-2 variants (2 μM) were pretreated with the indicated concentrations of naproxen, flurbiprofen, and diclofenac at 37 °C for 30 min and then assayed for COX activity with 100 μM AA using an O_2 electrode as described under "Experimental Procedures." Results are shown for a single experiment involving triplicate determinations. The *error bars* indicate the average ± S.E. Control values for each enzyme variant are normalized to 100%. A significant difference from the value with the Native/Native *versus* Y385F S121P/Native as determined by the Student's *t* test ($p < 0.05$) is indicated with an *asterisk*.

TABLE 6

Kinetic properties of variant forms of huPGHS-2 having substitutions of Arg-44 or Asp-125

huPGHS-2 variants were prepared and purified, and COX activities were assayed using an O_2 electrode as described under "Experimental Procedures." Kinetic values are from the average of triplicate determinations ± S.D. Appropriate control values (first three rows) and some comparators (*e.g.* R120A substitutions, Y385F R120A/Native huPGHS-2 cannot bind FAs efficiently) are from Ref. 9. * denotes a significant difference in V_{max} from His_8-native/ His_8-native huPGHS-2. § denotes a significant difference in V_{max} from His_8-Y385F/FLAG-native huPGHS-2.

huPGHS-2 variant (E_{allo}/E_{cat})	V_{max}	V_{max}	K_m	% activity with PA relative to control	Relative response to naproxen
	units /mg	*% of relevant control*	μM		
His_8-native/FLAG-native[a]	42 ± 2.0	100	12 ± 1.9	ND	Unchanged[b]
His_8-native/ His_8-native[a]	43 ± 2.0	100	9.3 ± 1.0	183 ± 1.0	Unchanged[b]
His_8-Y385F/FLAG-native[a]	37 ± 1.3	100	5.5 ± 0.8	146 ± 3.0	Unchanged[b]
His_8-Y385F R120A/FLAG-native[a]	16 ± 0 .5[§]	43	10 ± 1.0	100 ± 8.7[a]	Attenuated[a,c]
His_8-Y385F/FLAG-R120A[a]	35 ± 3.9	95	57 ± 15	122 ± 4.1[a]	Attenuated[a,c]
His_8-R120A/His_8-R120[a]	24 ± 0.6*	56	39 ± 2.8	91 ± 6.2[a]	Attenuated[a,b]
His_8-Y385F D125A/FLAG-native	21.6 ± 0.6[§]	59	11.6 ± 1.2	114 ± 4.9	Attenuated[c]
His_8-Y385F/FLAG-D125A	25.8 ± 0.9[§]	70	10.8 ± 1.3	141 ± 3.7	Unchanged[c]
His_8-D125A/His_8-D125A	27.9 ± 1.1*	65	9.8 ± 1.4	123 ± 3.6	Attenuated[b]
His_8-Y385F D125P/FLAG-native	11.2 ± 0.3[§]	30	6.9 ± 0.5	136 ± 2.2	Attenuated[c]
His_8-Y385F/FLAG-D125P	12.1 ± 0.3[§]	32	4.0 ± 0.3	137 ± 2.8	Unchanged[c]
His_8-D125P/His_8-D125P	18.6 ± 0.5*	43	10.2 ± 0.9	117 ± 10	Attenuated[b]
His_8-Y385F R44A/FLAG-native	8.8 ± 0.2[§]	24	5.6 ± 0.6	108 ± 12	Attenuated[c]
His_8-Y385F/FLAG-R44A	9.2 ± 0.3[§]	24	12.3 ± 1.5	126 ± 12	Unchanged[c]
His_8-R44A/His_8-R44AA	14.7 ± 1.8*	34	14.7 ± 0.6	108 ± 12	Attenuated[b]
His_8-Y385F R44Q/FLAG-native	16.4 ± 0.7[§]	43	5.2 ± 0.98	121 ± 11	Unchanged[c]
His_8-Y385F/FLAG-R44Q	21.3 ± 1.1[§]	57	13.8 ± 2.6	132 ± 9.0	Unchanged[c]
His_8-R44Q/His_8-R44Q	20.6 ± 0.8*	48	9.1 ± 1.3	95 ± 6.5	Attenuated[b]

[a] Values are from Ref. 9.
[b] Data are compared with Native/Native huPGHS-2.
[c] Data are compared with Y385F/Native huPGHS-2.

edly reduced from control values. These observations suggest that the Asp-125 to Arg-44 hydrogen bond is not critical for the functioning of PGHS-2.

Discussion

The rate-limiting step in COX catalysis is incompletely resolved but involves control over the distance between and/or relative orientation of the 13-pro-*S*-hydrogen of AA and the Tyr-385 radical or in some cases the stability of the Tyr-385 radical in E_{cat} (1, 3, 31). The E_{cat} subunit of PGHSs provides a readout of the allosteric effects of ligand binding to E_{allo} (10, 12). In this study, we have investigated the mechanistic basis for COX-2 allosteric regulation. Most importantly, we have provided new evidence that Arg-120 and the region immediately downstream of Arg-120 in E_{allo} involving residues 121–129 of huPGHS-2 mediates allosteric responses to FAs and allosteric COX inhibitors.

Allosteric Regulation and Tonic Inhibition of PGHS-2 Involving E_{allo}—As illustrated by the data in Table 5, huPGHS-2 is tonically inhibited when no ligands are bound to E_{allo}. Specifically, the V_{max} of purified recombinant huPGHS-2 without FA bound to Arg-120 of E_{allo} (*i.e.* with R120A Y385F/Native huPGHS-2) is 16 units/mg with AA as substrate. The V_{max}, again with AA as substrate, is increased to 37 units/mg with AA bound to E_{allo} (*i.e.* with Y385F/Native huPGHS-2). Thus, when bound to E_{allo}, AA itself allosterically activates E_{cat} toward the parent substrate AA.

Allosteric effects on huPGHS-2 that involve ligand binding and/or mutations to E_{allo} can modulate the V_{max} for human COX-2 activity over at least a 20-fold range from ~5–85 units/mg. At the lower end, the allosteric inhibitor FBP bound to E_{allo} causes more than 90% (albeit incomplete) inhibition. This is equivalent to an enzyme having a V_{max} of <5 units/mg (9, 14). At the other extreme one can estimate a V_{max} of 86 units/mg for S121P Y385F/Native huPGHS-2 when tested with 25 μM PA

plus 5 μM AA. This latter value underestimates the maximal activation by PA because E_{allo} is less than 50% occupied by PA (*versus* AA) under these conditions.

Potencies and Efficacies of Allosteric FA Activators and COX-2 Inhibitors—Many but not all FAs are capable of binding E_{allo}. This includes most saturated and monounsaturated FAs, which all bind with similar but relatively low affinities (*i.e.* K_d values of 5–10 μM) but exhibit different efficacies (9, 14). PA, the most efficacious common FA activator, causes a maximal allosteric activation that is 2–3 times greater than observed with AA alone, whereas maximal activation by stearate is 1.2-fold (11). Dihomo-γ-linolenic, AA, and EPA bind with relatively high and comparable affinities to E_{allo} (*i.e.* K_d values of ~0.25 μM (11)). Other 18, 20, and 22 carbon polyunsaturated FAs (11), 2-arachidonylglycerol, and 2-*O*-arachidonylglycerol ether bind poorly to E_{allo} (10, 12).

Allosteric COX-2 inhibitors also differ in their allosteric potencies and efficacies. IBP (functioning allosterically (12)), naproxen, and FBP cause about 50, 70, and 90% maximal inhibition, respectively, of AA oxygenation by native huPGHS-2 (and Y385F/Native huPGHS-2) (9, 12, 14). As noted above, when AA is unable to bind to E_{allo}, the enzyme has ~55% less activity than when AA is bound to E_{allo} (9). This implies that IBP, which causes ~50% inhibition via E_{allo} (12), simply prevents AA binding to E_{allo} without exerting an independent allosteric inhibitory effect. In contrast, the >90% inhibition seen with FBP must involve both prevention of AA binding and a significant additional allosteric inhibitory component. Naproxen, which causes about 70% maximal inhibition, must prevent AA binding to E_{allo} and also have a modest additional allosteric inhibitory component.

Repositioning of Residues 120–129 in E_{allo} Is Associated with COX-2 Allosterism—Previous studies have established the involvement of Arg-120 in E_{allo} in the allosteric responses of PGHS-2 to saturated, monounsaturated, and certain polyunsaturated FAs as well as to the allosteric COX inhibitors IBP, FBP, and naproxen (9, 11, 12). It is also known that loop residues 123–127 can assume two alternative configurations in X-ray crystal structures of ovine PGHS-1 (7, 28). Additionally, cross-linking studies with huPGHS-2 demonstrate that changes in the relative positions of residues 123–127 and 541–543 occur in association with the binding of some ligands to the COX sites (5). Specifically, cross-linking is affected by certain 20-carbon FAs, including AA and EPA, and many COX inhibitors, including FBP and IBP, that can bind at low micromolar concentrations to both E_{allo} and E_{cat} (5, 11). In contrast and importantly, 2-arachidonoylglycerol and FAs such as PA, oleic acid, linoleic acid, and docosahexaenoic acid that bind efficiently to only one of the two huPGHS-2 subunits do not affect cross-linking (5, 11).

The combination of crystallographic and cross-linking studies reported here indicate that the S121P mutations in S121P/S121P PGHS-2 cause the entire segment involving residues 119–129 to become "unhinged" from the N-terminal end of helix D of the membrane binding domain. This occurs in parallel with a substantial increase in enzyme activity that can be chiefly ascribed to the S121P substitution in E_{allo}. This S121P substitution largely compensates for ligand binding to E_{allo}. Thus, in comparing enzymes having E_{allo} subunits unable to bind ligands, we find that incorporating the S121P substitution in E_{allo} causes greater than a 3-fold increase in the V_{max} (*i.e.* comparing R120A S121P Y385F/Native *versus* R120A Y385F/Native huPGHS-2). We conclude that the S121P substitution leads to a large increase in the flexibility of the segment from Arg-120 to residue 129 of the adjoining allosteric loop in E_{allo} and that movement in this region of E_{allo} underlies the allosteric effects mediated by FAs and allosteric inhibitors that bind E_{allo}.

There is also evidence that movement of residues between 120 and 129 in E_{cat} occur upon ligand binding to this subunit and that these changes also contribute to COX allosterism. We infer that there is an E_{cat} contribution based (*a*) on previous studies showing that only ligands that can bind to E_{allo} and E_{cat} simultaneously at micromolar concentrations affect cross-linking (5, 11) and (*b*) on observations reported here that S121P and various Arg-44 and Asp-125 substitutions in E_{cat} have significant effects on COX activity.

Browner and co-workers (37) published the crystal structures of huPGHS-2 in complex with two inhibitors, RS104897 and RS57067, derived from a scaffold of the nonselective NSAID zomepirac. RS104897 bound in the COX channel in a similar fashion to that observed for other NSAIDs, with Arg-120, Tyr-355, and Glu-524 forming interactions to close the aperture of the channel. However, the binding of RS57067 captured the COX channel entrance in an "open" conformation. In the open conformation, Arg-120 no longer interacts with the carboxylate group of Glu-524. Instead, the side chain of Glu-524 reorients, forming an ionic interaction with Arg-513 at the base of the side pocket. Arg-120 no longer participates in the interaction network because the pyridazinone ring of RS57067 displaces Arg-120 causing helix D to become detached from the catalytic domain. The α-carbon of Arg-120 moves 2.3 Å compared with its position in the closed conformation. To date, this is the only COX crystal structure that exhibits a change in the interaction network at the channel entrance. Unfortunately, the coordinates for the complex were never deposited in the PDB. Nevertheless, the report of the unwinding of helix D provoked by the binding of RS57067 suggests that the structural conformation of the main chain observed in the S121P/apo-crystal structure represents a transient conformation that can be sampled by native enzyme.

Changes in Allosteric Responses with S121P Substitutions—Presumably, the degree and manner in which the allosteric loop interacts with the partner E_{cat} subunit are what modulates E_{cat} activity. The pattern of stimulatory effects of PA > oleic acid ~ 11-*cis*-eicosaenoic acid are similar for native huPGHS-2, Y385F/Native huPGHS-2, and S121P/S121P huPGHS-2. The S121P mutation in E_{allo} increases the flexibility of the allosteric loop while maintaining to some degree the overall specificity of nsFA activation. In contrast, oleic acid and 11-*cis*-eicosaenoic acid are equal to or better than PA in stimulating that activity of mutants with Arg-44, Asp-125, and Ala-543 mutations. These results reinforce the idea that each different nsFA when bound to E_{allo} must cause a subtly different alteration in or repositioning of the allosteric loop.

The inhibitory responses to FBP and naproxen were blunted by having the S121P substitution in E_{allo} but were unaffected

when this substitution was present in E_{cat}. The binding of the allosteric inhibitor FBP to S121P/S121P muPGHS-2 in crystal structures realigns residues 119–122 into positions observed in native muPGHS-2. One would expect a similar realignment in solution, along with realignment of residues 123–129 of the allosteric loop. Thus, it was somewhat surprising to us that S121P Y385F/Native huPGHS-2 would exhibit significantly attenuated responses to the allosteric inhibitors FBP and naproxen. We expected, for example, that FBP and probably naproxen binding would realign the structure of the E_{allo} subunit in S121P Y385F/Native huPGHS-2 to forms that would cause the same degrees of inhibition as observed with native enzyme (Fig. 8) or Y385F/Native huPGHS-2 (9). One possibility is that the X-ray structures are providing a view of what happens in E_{cat} but not in E_{allo} in solution. Perhaps only a partial realignment is occurring in E_{allo}, one that yields only incomplete responses to both activating and inhibitory ligands. This would be consistent with the observation that the magnitude of the effect of the S121P mutation on COX activation is reduced but not eliminated in the presence of AA binding to E_{allo} as discussed above.

Although it is clear from *in vitro* studies that COX-2 activity can be regulated allosterically by FAs and allosteric COX inhibitors, the physiologic significance of allosterism in COX-2 regulation remains to be explored. Changes in PG biosynthesis are observed in animals fed fish oil FAs (42), but these changes could arise from changes in substrate levels or other effects rather than allosterism. There is also a difference between naproxen and other nonspecific NSAIDS and COX-2 inhibitors in their cardiovascular profiles (43), but no data of which we are aware comparing naproxen and other inhibitors for their effects on PG formation *in vivo*.

Experimental Procedures

Materials—Arachidonic acid (AA) and oleic acid (18:1ω9) were purchased from Cayman Chemical Co. Nickel-nitrilotriacetic acid Superflow resin and nickel-nitrilotriacetic acid were from Qiagen. Flurbiprofen, indomethacin, aspirin, naproxen, 11-*cis*-eicosaenoic acid (20:1ω9), FLAG peptide, and FLAG affinity resin were from Sigma. Celebrex® (celecoxib) was from physician samples. Ibuprofen was from Tocris Bioscience. Hemin was from Frontier Scientific, Logan, UT. Co^{3+}-protoporphyrin IX was purchased from Frontier Scientific. BCA protein reagent was from Pierce. Polyacrylic acid (sodium salt) 5100 was from Hampton Research Corp. [1-^{14}C]AA (1.85 GBq/mmol) was from American Radiolabeled Chemicals. C10E6 and decyl maltoside were purchased from Anatrace (Maumee, OH). *N*-Octyl β-D-glucopyranoside (βOG) was purchased from Inalco (San Luis Obispo, CA). Hexane, isopropyl alcohol, and acetic acid were HPLC grade from Thermo Fisher Scientific, Inc. Complete protease inhibitor was from Roche Applied Science. Restriction enzymes were from New England Biolabs, Inc. All other materials were analytic grade from Sigma.

The QuikChange™ mutagenesis kit was purchased from Stratagene (La Jolla, CA). The Bac-to-Bac baculovirus expression kit and associated reagents, including fungizone and penicillin/streptomycin, were purchased from Invitrogen. Fetal bovine serum, *Spodoptera frugiperda* 21 (*Sf*21) insect cells, and ESF 921 protein-free insect cell media were purchased from Expression Systems (Davis, CA). HiTrap HP chelating and HiPrep Sephacryl 300-HR chromatography columns were purchased from GE Healthcare.

Preparation of Mutants—huPGHS-2 homodimers were prepared as detailed previously (9). A mutant protein variant denoted S121P/S121P huPGHS-2 indicates a variant in which both monomers of the huPGHS-2 dimer bear this mutation. Heterodimers were prepared as described in previous reports (4, 44) or using the pFastBac dual vector (9). A PGHS-2 variant denoted S121P/Native huPGHS-2 indicates a variant in which one monomer of the huPGHS-2 heterodimer bears the S121P mutation, and the other monomer has the native sequence. A cDNA for huPGHS-2 containing an octahistidine (His_8) tag at the N terminus was subcloned into pFastBac plasmid (Invitrogen)). The QuikChange site-directed mutagenesis protocol (Stratagene) was used to construct the mutants. The presence of the various mutations was confirmed by DNA sequencing. Native huPGHS-2, mutant huPGHS-2 homodimers, and heterodimeric huPGHS-2 variants were expressed and purified using procedures described previously (9).

Cyclooxygenase Analyses—COX activities were determined using measurements of O_2 consumption using an O2 electrode essentially as detailed previously (9). In experiments involving COX inhibitors, the enzyme preparations were typically preincubated with the inhibitor, and an aliquot was added to the reaction chamber. The rates reported are maximal rates occurring after about a 10-s lag phase.

Difference absorption spectra of the S121P/S121P huPGHS-2 homodimer were obtained upon titration with heme, and K_d values for heme and heme binding stoichiometry were calculated as described previously (9, 14, 15).

Quantitation of the binding of [1-^{14}C]AA to E_{allo} of various homodimers and heterodimers at high enzyme to substrate ratios was as described in earlier reports (9, 11, 14, 15).

Cyclooxygenase product analyses were conducted in 100-μl reaction mixtures containing 1 μM [1-^{14}C]AA, 0.10–2.0 μM huPGHS-2 or mutant variants, 5 μM hematin and 1 mM phenol in 0.1 M Tris-HCl, pH 8.0, at 37 °C. The reactions were quenched with 100 μl of stop buffer consisting of ethyl acetate/acetic acid (95:5; v/v). The resultant samples were centrifuged at room temperature for 5 min at 4000 × *g*. An aliquot of the organic layer (100 μl) was subjected to HPLC on a Luna C18 (2) column (5 μm, 250 × 4.6 mm, Phenomenex) mounted on a Shimadzu HPLC system equipped with radio-HPLC detector (IN/US system, β-RAM model 4). The bound products were eluted in a gradient elution mode eluting with Solution A (acetonitrile/water; 30:70) for 5 min and then with a linear gradient of Solutions A and B (acetonitrile/water; 90:10) for 15 min, then Solution B for 8 min, and finally Solution A for 4 min; Solutions A and B both contained 0.1% acetic acid (v/v). The flow rate was 1 ml/min. Representative elution times for PGH2, 17-hydroxyheptadecatrienoic acid, and AA were 14, 18, and 30 min, respectively. Prostaglandin product analysis was determined using the same methods as those used for measuring [1-^{14}C]AA binding to E_{allo} except that incubations were performed with 50 μM [1-^{14}C]AA instead of 1 μM [1-^{14}C]AA and 300 nM huPGHS-2 and mutant huPGHS-2 variants.

Statistical Analyses—Student's *t* tests were performed in Microsoft Excel. If the experiments had the same numbers of repetitions, probabilities were calculated with a Student's paired *t* test, with a two-tailed distribution. If the experiments had different numbers of repetitions, probabilities were calculated with a Student's unequal variance *t* test, with a two-tailed distribution.

Oxidant-induced Disulfide Cross-linking between Monomers of huPGHS-2—Before cross-linking, the PGHS-2 variants containing cysteine substitutions (1 μM monomer) (*i.e.* P127C S541C Δ*C*-huPGHS-2, R120Q P127C S541C Δ*C*-huPGHS-2, and S121P P127C S541C Δ*C*-huPGHS-2) were reconstituted with a 1.5 M excess of Co^{3+}-protoporphyrin IX. Cross-linking to form disulfide bonds was initiated by making the solution 250 μM Cu(II)/(1,10-phenathroline)$_3$ (*i.e.* 250 μM $CuSO_4$ plus 625 μM 1,10-phenathroline) at room temperature for various times. To test the effect of FBP on cross-linking, the proteins were pre-incubated with FBP for 10 min before addition of the Cu(II)/*o*-phenanthroline oxidant. The reactions were stopped by adding SDS-loading buffer (Invitrogen) containing 20 mM *N*-ethylmaleimide and 20 mM EDTA (and no reductants). The reaction mixtures were then subjected to SDS-PAGE, and immunoblotting was performed with a rabbit polyclonal antibody reactive with against huPGHS-2 as detailed previously (45).

Crystallography—The S121P mutation in muPGHS-2 was generated using the QuikChange mutagenesis kit and the previously engineered His_6-N580A muPGHS-2 in pFastBac1 (27) as the template. This protein variant is denoted S121P/S121P muPGHS-2 to indicate that both monomers of the dimer bear this mutation. Expression and purification of S121P/S121P muPGHS-2 for structural characterization was carried out as described previously (27). Prior to crystallization, purified S121P/S121P muPGHS-2 was concentrated to 3.3 mg/ml using a 50-kDa MWCO centrifugal concentrator (Millipore) and reconstituted with a 2-fold mole excess of Co^{3+}-protoporphyrin IX to generate the holoenzyme. Crystals were grown at 23 °C using the sitting drop vapor diffusion method by mixing 3 μl of protein solution with 3 μl of a solution consisting of 23–34% polyacrylic acid 5100, 100 mM HEPES, pH 7.5, 20 mM $MgCl_2$, and 0.6% (w/v) βOG. Drops were then equilibrated over reservoir solutions containing 23–34% polyacrylic acid 5100, 100 mM HEPES, pH 7.5, and 20 mM $MgCl_2$. For diffraction analysis, crystals were flash-frozen directly in the gaseous nitrogen stream after soaking in drop solution supplemented with 10% ethylene glycol. To generate inhibitor-bound structures, crystals were soaked in the above cryoprotectant that also contained 1 mM inhibitor for 20 min prior to flash freezing. X-ray diffraction data were collected on beamline 17-ID at the Advanced Photon Source (Argonne National Laboratory) using a Pilatus 6M detector and processed with HKL2000 (46). Data collection statistics are reported in Table 4.

Molecular replacement methods were used to determine the initial phases for each structure, with an emphasis on minimizing the introduction of model bias as described previously (27). A truncated search model of muCOX-2 derived from PDB entry 3HS5 was utilized in PHASER (47). Subsequent phases obtained from PHASER were input into ARP/wARP utilizing the "automated model building starting from experimental phases" option (48), which successfully built most of the deleted portions of the models. Iterative cycles of model building and refinement, using COOT (49) and PHENIX (50), were then implemented to fit the remaining residues and to add waters, inhibitors, and other ligand molecules. Translation-libration-screw (TLS) refinement (51), utilizing the TLSMD web server (52, 53) was carried out during the final rounds of refinement. Final refinement statistics are summarized in Table 4. Model validation was carried out using MolProbity (54) and simulated annealing omit maps were calculated in PHENIX. The coordinates and structure factors for S121P/apo, S121P/cbx, and S121P/fbp have been deposited in the Protein Data Bank (PDB codes 5JVY, 5JW1, and 5JVZ, respectively).

Thermal Shift Assay—Thermal shift assays were performed using a Stratagene Mx3005P real time PCR instrument and the thiol reactive fluorescent dye 7-diethylamino-3-(4′-maleimidylphenyl)-4-methylcoumarin (CPM) (55). Native, R120A (29), and S121P/S121P muPGHS-2 were added to a final concentration of 1 μM in a 30-μl total reaction volume containing 25 mM Tris-HCl, pH 8.0, 150 mM NaCl, and 0.53% (w/v) βOG. To analyze inhibitor binding, 50 μM of either FBP, naproxen, or celecoxib, or 100 μM IBP was added to the reaction, followed by incubation on ice for 30 min. CPM was then added to a final concentration of 25 μM. The change in fluorescence was monitored using an Alexa filter with excitation and emission wavelengths of 350 and 440 nm, respectively. Temperature was raised from 25 to 98 °C in 0.5 °C increments over the course of 45 min, with fluorescence readings taken at each interval. The fluorescence data were plotted and normalized, and the first derivative of the curve was calculated to provide the T_m. The change in melting temperature (ΔT_m) was calculated as the difference between the T_m of the native or mutant construct in the presence of inhibitor compared with the native or mutant construct alone.

Author Contributions—L. D. and C. Y. prepared and characterized huPGHS-2 mutants and contributed to the data analyses and writing of the manuscript. B. J. O. and M. G. M. carried out X-ray crystallographic structure determinations and thermal melting temperature experiments. W. L. S. and the other authors were involved in experimental design, data analysis, and writing of the manuscript.

Acknowledgments—X-ray diffraction experiments were conducted on IMCA-CAT beamline 17-ID at the Advanced Photon Source, which is supported by companies of the Industrial Macromolecular Crystallography Association through a contract with the Hauptman-Woodward Medical Research Institute.

References

1. Tsai, A. L., and Kulmacz, R. J. (2010) Prostaglandin H synthase: resolved and unresolved mechanistic issues. *Arch. Biochem. Biophys.* **493,** 103–124
2. Smith, W. L., Urade, Y., and Jakobsson, P. J. (2011) Enzymes of the cyclooxygenase pathways of prostanoid biosynthesis. *Chem. Rev.* **111,** 5821–5865
3. Liu, Y., and Roth, J. P. (2016) A revised mechanism for human cyclooxygenase-2. *J. Biol. Chem.* **291,** 948–958
4. Yuan, C., Rieke, C. J., Rimon, G., Wingerd, B. A., and Smith, W. L. (2006) Partnering between monomers of cyclooxygenase-2 homodimers. *Proc. Natl. Acad. Sci. U.S.A.* **103,** 6142–6147

5. Yuan, C., Sidhu, R. S., Kuklev, D. V., Kado, Y., Wada, M., Song, I., and Smith, W. L. (2009) Cyclooxygenase allosterism, fatty acid-mediated cross-talk between monomers of cyclooxygenase homodimers. *J. Biol. Chem.* **284,** 10046–10055
6. Prusakiewicz, J. J., Duggan, K. C., Rouzer, C. A., and Marnett, L. J. (2009) Differential sensitivity and mechanism of inhibition of COX-2 oxygenation of arachidonic acid and 2-arachidonoylglycerol by ibuprofen and mefenamic acid. *Biochemistry* **48,** 7353–7355
7. Rimon, G., Sidhu, R. S., Lauver, D. A., Lee, J. Y., Sharma, N. P., Yuan, C., Frieler, R. A., Trievel, R. C., Lucchesi, B. R., and Smith, W. L. (2010) Coxibs interfere with the action of aspirin by binding tightly to one monomer of cyclooxygenase-1. *Proc. Natl. Acad. Sci. U.S.A.* **107,** 28–33
8. Sharma, N. P., Dong, L., Yuan, C., Noon, K. R., and Smith, W. L. (2010) Asymmetric acetylation of the cyclooxygenase-2 homodimer by aspirin and its effects on the oxygenation of arachidonic, eicosapentaenoic, and docosahexaenoic acids. *Mol. Pharmacol.* **77,** 979–986
9. Dong, L., Sharma, N. P., Jurban, B. J., and Smith, W. L. (2013) Pre-existent asymmetry in the human cyclooxygenase-2 sequence homodimer. *J. Biol. Chem.* **288,** 28641–28655
10. Kudalkar, S. N., Nikas, S. P., Kingsley, P. J., Xu, S., Galligan, J. J., Rouzer, C. A., Banerjee, S., Ji, L., Eno, M. R., Makriyannis, A., and Marnett, L. J. (2015) 13-Methylarachidonic acid is a positive allosteric modulator of endocannabinoid oxygenation by cyclooxygenase. *J. Biol. Chem.* **290,** 7897–7909
11. Dong, L., Zou, H., Yuan, C., Hong, Y. H., Kuklev, D. V., and Smith, W. L. (2016) Different fatty acids compete with arachidonic acid for binding to the allosteric or catalytic subunits of cyclooxygenases to regulate prostanoid synthesis. *J. Biol. Chem.* **291,** 4069–4078
12. Dong, L., Zou, H., Yuan, C., Hong, Y. H., Uhlson, C. L., Murphy, R. C., and Smith, W. L. (2016) Interactions of 2-*O*-arachidonylglycerol ether and ibuprofen with the allosteric and catalytic subunits of human COX-2. *J. Lipid Res.* **57,** 1043–1050
13. Kulmacz, R. J., and Lands, W. E. (1984) Prostaglandin H synthase. Stoichiometry of heme cofactor. *J. Biol. Chem.* **259,** 6358–6363
14. Dong, L., Vecchio, A. J., Sharma, N. P., Jurban, B. J., Malkowski, M. G., and Smith, W. L. (2011) Human cyclooxygenase-2 is a sequence homodimer that functions as a conformational heterodimer. *J. Biol. Chem.* **286,** 19035–19046
15. Zou, H., Yuan, C., Dong, L., Sidhu, R. S., Hong, Y. H., Kuklev, D. V., and Smith, W. L. (2012) Human cyclooxygenase-1 activity and its responses to COX inhibitors are allosterically regulated by nonsubstrate fatty acids. *J. Lipid Res.* **53,** 1336–1347
16. Smith, W. L., DeWitt, D. L., and Garavito, R. M. (2000) Cyclooxygenases: structural, cellular and molecular biology. *Annu. Rev. Biochem.* **69,** 149–182
17. Picot, D., Loll, P. J., and Garavito, R. M. (1994) The X-ray crystal structure of the membrane protein prostaglandin H2 synthase-1. *Nature* **367,** 243–249
18. Kurumbail, R. G., Stevens, A. M., Gierse, J. K., McDonald, J. J., Stegeman, R. A., Pak, J. Y., Gildehaus, D., Miyashiro, J. M., Penning, T. D., Seibert, K., Isakson, P. C., and Stallings, W. C. (1996) Structural basis for selective inhibition of cyclooxygenase-2 by anti-inflammatory agents. *Nature* **384,** 644–648
19. Spencer, A. G., Thuresson, E., Otto, J. C., Song, I., Smith, T., DeWitt, D. L., Garavito, R. M., and Smith, W. L. (1999) The membrane binding domains of prostaglandin endoperoxide H synthase-1 and -2: Peptide mapping and mutational analysis. *J. Biol. Chem.* **274,** 32936–32942
20. Mancini, J. A., Riendeau, D., Falgueyret, J. P., Vickers, P. J., and O'Neill, G. P. (1995) Arginine 120 of prostaglandin G/H synthase-1 is required for the inhibition by nonsteroidal anti-inflammatory drugs containing a carboxylic acid moiety. *J. Biol. Chem.* **270,** 29372–29377
21. Bhattacharyya, D. K., Lecomte, M., Rieke, C. J., Garavito, M., and Smith, W. L. (1996) Involvement of arginine 120, glutamate 524, and tyrosine 355 in the binding of arachidonate and 2-phenylpropionic acid inhibitors to the cyclooxygenase active site of ovine prostaglandin endoperoxide H synthase-1. *J. Biol. Chem.* **271,** 2179–2184
22. Malkowski, M. G., Ginell, S. L., Smith, W. L., and Garavito, R. M. (2000) The X-ray crystal structure of prostaglandin endoperoxide H synthase-1 complexed with arachidonic acid. *Science* **289,** 1933–1937
23. Malkowski, M. G., Theisen, M. J., Scharmen, A., and Garavito, R. M. (2000) The formation of stable fatty acid substrate complexes in prostaglandin H2 synthase-1. *Arch. Biochem. Biophys.* **380,** 39–45
24. Malkowski, M. G., Thuresson, E. D., Lakkides, K. M., Rieke, C. J., Micielli, R., Smith, W. L., and Garavito, R. M. (2001) Structure of eicosapentaenoic and linoleic acids in the cyclooxygenase site of prostaglandin endoperoxide H synthase-1. *J. Biol. Chem.* **276,** 37547–37555
25. Thuresson, E. D., Lakkides, K. M., Rieke, C. J., Sun, Y., Wingerd, B. A., Micielli, R., Mulichak, A. M., Malkowski, M. G., Garavito, R. M., and Smith, W. L. (2001) Prostaglandin endoperoxide H synthase-1: the functions of cyclooxygenase active site residues in the binding, positioning, and oxygenation of arachidonic acid. *J. Biol. Chem.* **276,** 10347–10357
26. Thuresson, E. D., Malkowski, M. G., Lakkides, K. M., Rieke, C. J., Mulichak, A. M., Ginell, S. L., Garavito, R. M., and Smith, W. L. (2001) Mutational and X-ray crystallographic analysis of the interaction of dihomo-gamma-linolenic acid with prostaglandin endoperoxide H synthases. *J. Biol. Chem.* **276,** 10358–10365
27. Vecchio, A. J., Simmons, D. M., and Malkowski, M. G. (2010) Structural basis of fatty acid substrate binding to cyclooxygenase-2. *J. Biol. Chem.* **285,** 22152–22163
28. Sidhu, R. S., Lee, J. Y., Yuan, C., and Smith, W. L. (2010) Comparison of cyclooxygenase-1 crystal structures: cross-talk between monomers comprising cyclooxygenase-1 homodimers. *Biochemistry* **49,** 7069–7079
29. Vecchio, A. J., Orlando, B. J., Nandagiri, R., and Malkowski, M. G. (2012) Investigating substrate promiscuity in cyclooxygenase-2: the role of Arg-120 and residues lining the hydrophobic groove. *J. Biol. Chem.* **287,** 24619–24630
30. Blobaum, A. L., Xu, S., Rowlinson, S. W., Duggan, K. C., Banerjee, S., Kudalkar, S. N., Birmingham, W. R., Ghebreselasie, K., and Marnett, L. J. (2015) Action at a distance: mutations of peripheral residues transform rapid reversible inhibitors to slow, tight binds of cyclooxyenase-2. *J. Biol. Chem.* **290,** 12793–12803
31. Orlando, B. J., and Malkowski, M. G. (2016) Substrate-selective inhibition of cyclooxygeanse-2 by fenamic acid derivatives is dependent on peroxide tone. *J. Biol. Chem.* **291,** 15069–15081
32. Vecchio, A. J., and Malkowski, M. G. (2011) The structural basis of endocannabinoid oxygenation by cyclooxygenase-2. *J. Biol. Chem.* **286,** 20736–20745
33. Garavito, R. M., Malkowski, M. G., and DeWitt, D. L. (2002) The structures of prostaglandin endoperoxide H synthases-1 and -2. *Prostaglandins Other Lipid Mediat.* **68,** 129–152
34. Vecchio, A. J., and Malkowski, M. G. (2011) The structure of NS-398 bound to cyclooxygenase-2. *J. Struct. Biol.* **176,** 254–258
35. Greig, G. M., Francis, D. A., Falgueyret, J. P., Ouellet, M., Percival, M. D., Roy, P., Bayly, C., Mancini, J. A., and O'Neill, G. P. (1997) The interaction of arginine 106 of human prostaglandin G/H synthase-2 with inhibitors is not a universal component of inhibition mediated by nonsteroidal anti-inflammatory drugs. *Mol. Pharmacol.* **52,** 829–838
36. Rieke, C. J., Mulichak, A. M., Garavito, R. M., and Smith, W. L. (1999) The role of arginine 120 of human prostaglandin endoperoxide H synthase-2 in the interaction with fatty acid substrates and inhibitors. *J. Biol. Chem.* **274,** 17109–17114
37. Luong, C., Miller, A., Barnett, J., Chow, J., Ramesha, C., and Browner, M. F. (1996) Flexibility of the NSAID binding site in the structure of human cylcooxygenase-2. *Nat. Struct. Biol.* **3,** 927–933
38. Duggan, K. C., Walters, M. J., Musee, J., Harp, J. M., Kiefer, J. R., Oates, J. A., and Marnett, L. J. (2010) Molecular basis for cyclooxygenase inhibition by the non-steroidal anti-inflammatory drug naproxen. *J. Biol. Chem.* **285,** 34950–34959
39. Orlando, B. J., Lucido, M. J., and Malkowski, M. G. (2015) The structure of ibuprofen bound to cyclooxygenase-2. *J. Struct. Biol.* **189,** 62–66
40. Wang, J. L., Limburg, D., Graneto, M. J., Springer, J., Hamper, J. R., Liao, S., Pawlitz, J. L., Kurumbail, R. G., Maziasz, T., Talley, J. J., Kiefer, J. R., and Carter, J. (2010) The novel benzopyran class of selective cyclooxygenase-2

inhibitors. Part 2: the second clinical candidate having a shorter and favorable human half-life. *Bioorg. Med. Chem. Lett.* **20,** 7159–7163
41. Duggan, K. C., Hermanson, D. J., Musee, J., Prusakiewicz, J. J., Scheib, J. L., Carter, B. D., Banerjee, S., Oates, J. A., and Marnett, L. J. (2011) (*R*)-Profens are substrate-selective inhibitors of endocannabinoid oxygenation by COX-2. *Nat. Chem. Biol.* **7,** 803–809
42. Jiang, Y., Djuric, Z., Sen, A., Ren, J., Kuklev, D., Waters, I., Zhao, L., Uhlson, C. L., Hong, Y. H., Murphy, R. C., Normolle, D. P., Smith, W. L., and Brenner, D. E. (2014) Biomarkers for personalizing *ω*-3 fatty acid dosing. *Cancer Prev. Res.* **7,** 1011–1022
43. Trelle, S., Reichenbach, S., Wandel, S., Hildebrand, P., Tschannen, B., Villiger, P. M., Egger, M., and Juni, P. (2011) Cardiovascular safety of non-steroidal anti-inflammatory drugs: network meta-analysis. *Br. Med. J.* **342,** c7086
44. Liu, J., Seibold, S. A., Rieke, C. J., Song, I., Cukier, R. I., and Smith, W. L. (2007) Prostaglandin endoperoxide H synthases: peroxidase hydroperoxide specificity and cyclooxygenase activation. *J. Biol. Chem.* **282,** 18233–18244
45. Mbonye, U. R., Yuan, C., Harris, C. E., Sidhu, R. S., Song, I., Arakawa, T., and Smith, W. L. (2008) Two distinct pathways for cyclooxygenase-2 protein degradation. *J. Biol. Chem.* **283,** 8611–8623
46. Otwinowski, Z., and Minor, W. (1997) Processing of X-ray diffraction data collected in oscillation mode. *Methods Enzymol.* **276,** 307–326
47. McCoy, A. J., Grosse-Kunstleve, R. W., Adams, P. D., Winn, M. D., Storoni, L. C., and Read, R. J. (2007) Phaser crystallographic software. *J. Appl Crystallogr.* **40,** 658–674
48. Langer, G., Cohen, S. X., Lamzin, V. S., and Perrakis, A. (2008) Automated macromolecular model building for X-ray crystallography using ARP/wARP version 7. *Nat. Protoc.* **3,** 1171–1179
49. Emsley, P., and Cowtan, K. (2004) Coot: model-building tools for molecular graphics. *Acta Crystallogr. D Biol. Crystallogr.* **60,** 2126–2132
50. Adams, P. D., Afonine, P. V., Bunkóczi, G., Chen, V. B., Davis, I. W., Echols, N., Headd, J. J., Hung, L. W., Kapral, G. J., Grosse-Kunstleve, R. W., McCoy, A. J., Moriarty, N. W., Oeffner, R., Read, R. J., Richardson, D. C., *et al.* (2010) PHENIX: a comprehensive Python-based system for macromolecular structure solution. *Acta Crystallogr. D. Biol. Crystallogr.* **66,** 213–221
51. Winn, M. D., Isupov, M. N., and Murshudov, G. N. (2001) Use of TLS parameters to model anisotropic displacements in macromolecular refinement. *Acta Crystallogr. D Biol. Crystallogr.* **57,** 122–133
52. Painter, J., and Merritt, E. A. (2006) Optimal description of a protein structure in terms of multiple groups undergoing TLS motion. *Acta Crystallogr. D Biol. Crystallogr.* **62,** 439–450
53. Painter, J., and Merritt, E. A. (2006) TLSMD web server for the generation of multi-group TLS models. *J. Appl. Crystallogr.* **39,** 109–111
54. Davis, I. W., Leaver-Fay, A., Chen, V. B., Block, J. N., Kapral, G. J., Wang, X., Murray, L. W., Arendall, W. B., 3rd., Snoeyink, J., Richardson, J. S., and Richardson, D. C. (2007) MolProbity: all-atom contacts and structure validation for proteins and nucleic acids. *Nucleic Acids Res.* **35,** W375–W383
55. Alexandrov, A. I., Mileni, M., Chien, E. Y., Hanson, M. A., and Stevens, R. C. (2008) Microscale fluorescent thermal stability assay for membrane proteins. *Structure* **16,** 351–359
56. Evans, E. J., Castro, M. A., O'Brien, R., Kearney, A., Walsh, H., Sparks, L. M., Tucknott, M. G., Davies, E. A., Carmo, A. M., van der Merwe, P. A., Stuart, D. I., Jones, E. Y., Ladbury, J. E., Ikemizu, S., and Davis, S. J. (2006) Crystal structure and binding properties of the CD2 and CD244 (2B4)-binding protein, CD48. *J. Biol. Chem.* **281,** 29309–29320
57. Karplus, P. A., and Diederichs, K. (2012) Linking crystallographic model and data quality. *Science* **336,** 1030–1033

Fatty Acid Binding to the Allosteric Subunit of Cyclooxygenase-2 Relieves a Tonic Inhibition of the Catalytic Subunit

Liang Dong, Chong Yuan, Benjamin J. Orlando, Michael G. Malkowski and William L. Smith

J. Biol. Chem. 2016, 291:25641-25655.
doi: 10.1074/jbc.M116.757310 originally published online October 18, 2016